Dynamic Characteristics of Periodic Motions in a Restricted N-Body Problem

Christos S. Tsironis

***Abstract*—We investigate the existence and follow the evolution and dynamic stability of periodic motions in a restricted version of the N-body problem, where the positions of the mass bodies reside persistently on a planar polygon ring and its geometrical centre. The results show the existence of both (linearly) stable and unstable periodic orbits around the body placed on the ring centre (inside the ring), around all the periphery bodies (outside the ring) and around one or more of the periphery bodies. The stable periodic trajectories form regions of gravitational stability, whereas some classes of the unstable orbits exhibit bifurcations to non-symmetric periodic orbits of the same period, and less often period-doubling bifurcations.**

***Index Terms*—Celestial Mechanics, N-body problem, periodic orbits, linear stability, bifurcations.**

I. Introduction

THE GEOMETRIC and dynamic complexity of motions in multi-body systems under the mutual gravitational forces is nowadays well identified after many years of corresponding research (see [1-4] and references therein). However, under certain circumstances, the simulation of such systems may be uncomplicated by using simpler N-body models based on geometrical properties of the system under study [5-7]. An example of such a simplification is the adoption of a planar N-body ring configuration: N-1 spherical bodies of equal mass, located on the acmes of a regular polygon that rotates with constant angular velocity around an immobile body, which is located on the polygon center and has b times larger mass than the one of the peripheral bodies [8-10].

In this paper, which is a continuation of previous relevant work in [11], we investigate the geometry and dynamics of the motion of a small body in the gravitational field of an N-body ring configuration for N=8 and b=2, concentrating on the classification, evolution and linear stability of several types of periodic orbits. From the existing two-dimensional periodic trajectories, the symmetric ones with respect to the horizontal axis of the synodic coordinate system are of much importance, since these surround the central body as well as one or more of the peripheral bodies, thus making a returning transition from the inner to the outer region of the polygon.

The paper was submitted for review to the Journal of Astronomical and Astrophysical Research on 14/9/2013.

C. S. Tsironis is with the School of Electrical and Computer Engineering, National Technical University of Athens, 15773 Athens, GR (e-mail: ctsiron@mail.ntua.gr) and the Department of Physics, Aristotle University of Thessaloniki, 54124 Thessaloniki, GR (e-mail: ctsironis@astro.auth.gr).

The numerical computations yield both (linearly) stable and unstable motions, which appear different dynamic evolution depending primarily on the initial conditions: A number of the orbits remain stable, and therefore regions of gravitational stability are formed, while some orbits are always unstable. Many of those unstable orbits are most probable to escape from the ring region, however there is a high probability for their trapping in one of the stability regions. We have also come upon cases where new families of orbits are generated, as a result of occurring bifurcations of the conventional type or period-doubling ones [12].

The selection of values for the parameters N and b has been influenced by a rough multi-body approximation of planetary systems having a central star of comparable size and the initial state of asteroid populations formed around small planets. The variation of all the aforementioned properties of the periodic motion as the mass ratio and the number of peripheral bodies changes are to be studied thoroughly within a future work. The general trend is that the computation of some of the classes of trajectories becomes more persistent as the number of bodies increases and the mass ratio decreases, because the possibility of collisions with the peripheral bodies becomes higher as their number increases and their gravitational force reaches values comparable to the force from the central body.

The structure of the paper is as follows: In Section II the equations of motion are presented and explained, whereas in Section III a theoretical analysis provides information which can be deducted without the need of numerical computations. Then, in Section IV the numerical results are presented, and finally in Section V a discussion is made on the implications of the results and the approximations of our model.

II. Problem Formulation

A planar N-body ring configuration consists of N-1bodies of equal mass m located on the acmes of a regular polygon, which will be mentioned as “peripherals” from now on, and a body of mass M=bm placed on the geometric center of the polygon, and called “primary” in the following. Regarding the ring system kinematics, the regular assumption that the gravitational forces on each one of the N bodies evens up the centrifugal force is adopted, which allows for circular motion of the peripherals around the primary with common constant angular velocity ω, and therefore for the preservation of the regularity of the polygon (for more details on this issue the reader is pointed to [6-9]).

DOI: 10.5176/2335-6901_1.2.10

For the aforementioned configuration, it is convenient to describe the motions in a synodic Cartesian coordinate system initiated at the common mass centre of the ring configuration. The coordinates of the peripherals in this system are

$$X_i = \frac{\cos[(i-1)\Theta]}{\sqrt{2(1-\cos\Theta)}} L, \quad Y_i = \frac{\sin[(i-1)\Theta]}{\sqrt{2(1-\cos\Theta)}} L, \tag{1}$$

where i=1,2,…,N-1,and L, Θ the two polygon constants: L is the polygon side (distance between two adjacent peripherals) and Θ=2π/N is the polygon angle. For the sake of simplicity, a transformation of the physical coordinates to a dimensionless set of coordinates is performed, using the relations

$$x_i = \frac{X_i}{L}, \quad y_i = \frac{Y_i}{L}, \quad t = \omega\tau, \tag{2}$$

with X_i, Y_i, τ the values of the Cartesian coordinates and time before transformation and x_i, y_i, t the dimensionless values.

The second law of Newton for the motion of a particle in a gravitational field, the mass of which may be considered negligible with respect to the mass generating the field, yields equations similar to the restricted three-body problem [1, 3]

$$\frac{dx}{dt} - 2\frac{dy}{dt} = \frac{\partial V}{\partial x}, \quad \frac{dy}{dt} + 2\frac{dx}{dt} = \frac{\partial V}{\partial y}. \tag{3}$$

The potential function V(x,y,r_i), which depends only on the spatial coordinates, is expressed in normalized units as

$$\mathrm{V} = \frac{1}{2}\left(x^2 + y^2\right) + \frac{1}{D}\left(\frac{b}{r_0} + \sum_{i=1}^{N-1}\frac{1}{r_i}\right). \tag{4}$$

In (4), r_0,…,r_i are the dimensionless distances of the small particle from the primary and the peripherals respectively

$$r_0 = \sqrt{x^2 + y^2}, \; r_i = \sqrt{\left(x - x_i\right)^2 + \left(y - y_i\right)^2}, \tag{5}$$

whereas D is a constant determined by the geometrical properties of the polygon [6-11]

$$\mathrm{D} = \sqrt{2(1-cos\Theta)}\left\{\sum_{i=2}^{N-1}\frac{\sin^2\left(\frac{\Theta}{2}\right)\cos\left|\left(\frac{N+1}{2}-i\right)\frac{\Theta}{2}\right|}{\sin^2\left[\left(N-i\right)\frac{\Theta}{2}\right]} + bM^2\right\}. \tag{6}$$

The integral of Jacobi for the equations of motion is

$$C = 2V - \left(\frac{dx}{dt}\right)^2 - \left(\frac{dy}{dt}\right)^2 = 2V - \left(\frac{d\mathbf{r}}{dt}\right)^2, \tag{7}$$

where C is referred to as the Jacobian constant.

In this study we have computed two-dimensional (lying on the same plane with the N-body system), direct and retrograde symmetric periodic trajectories, by performing a numerical integration of the equations of motion using a fourth-order Runge-Kutta method [13]. Among all the orbits, of particular interest are the symmetric ones with respect to the rotating axis joining the central primary with one of the peripherals, which in our choice of coordinates is labelled as the x-axis. The corresponding particles are launched perpendicularly to the x-axis on the physical plane x-y with initial conditions all equal to zero: $x_0 = 0,\ y_0 = 0,\ dx_0/dt = 0,\ dy_0/dt = 0$.

The linear stability is determined by evaluating the Henon indices a_1, a_2, a_3, a_4, which are functions of the initial values x_0, dx_0/dt and C [14]. In this description, orbits are stable if $|a_1+a_4|<2$, but the existence of symmetry ($a_1=a_4$) simplifies the stability condition to $|a_1|<1$. When $|a_1|$ crosses 1 and $a_2a_3<0$ a regular ($a_2>0$) or period-doubling ($a_2<0$) bifurcation occurs. The numerical accuracy in the computation of the Henon indices is verified against the condition that the Jacobian determinant is equal to one ($a_1a_4-a_2a_3=1$). Due to the symmetry of the periodic orbits under study, it is possible to evaluate the stability indices based only on half the total orbit, and so the overall computation is significantly expedited [14, 15].

III. Theoretical Investigation

In this section we make a theoretical analysis of the dynamic system described above, with the scope of providing a qualitative picture of the motion of the small particle in the N-body ring potential, under a number of approximations, and obtaining a first estimation of the system dynamics before launching the numerical computation of the orbits.

A first step for the analysis and classification of orbits is to construct a map of the allowable regions of motion in real space. This is done in terms of determining a specific class of equipotential curves of the system, the ones where the kinetic energy vanishes [16, 17]. From (7) one sees that for given values of the Jacobian constant, it is feasible to construct curves in the x-y plane on which V=C/2 and the velocity vanishes. If such a zero-velocity curve is closed, the particle cannot escape from its interior if placed there with initial conditions based on the value of C used to construct the curve, hence the (energetically) allowed region of motion is defined. The exact mathematical formula for such a region may be derived from (4) for the specific value of the potential

$$x^2 + y^2 + \frac{2b}{D}\left(\frac{1}{\sqrt{x^2+y^2}} + \sum_{i=1}^{N-1}\frac{1}{\sqrt{\left(x-x_i\right)^2 + \left(y-y_i\right)^2}}\right) \geq C. \tag{8}$$

In Fig. 1 the zero-velocity curves for the system under study (N-body ring with N=8, b=2) are visualized. According to the specific picture, three classes of orbits are immediately identified: One around the primary, one around a peripheral and one around all ring bodies. Those are the simplest types of motions from the ones to be computed later on.

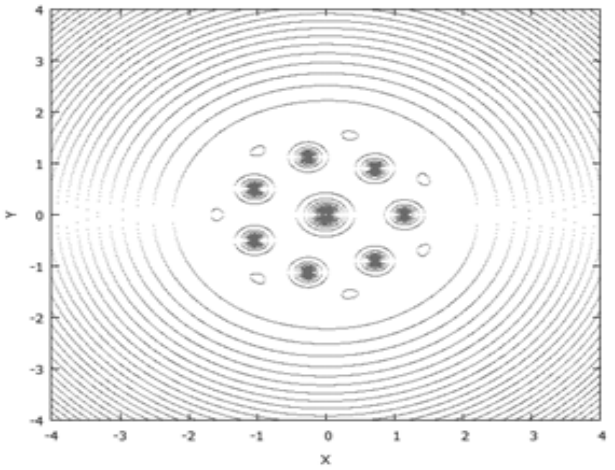

Fig. 1. Zero-velocity curves in real space for the system under study.

In the region far from the ring polygon, the description of periodic motions in the sidereal coordinate system may be simplified because, due to the symmetry of the problem, the force on the moving particle can be approximately considered as Kepler-like, resulting to a motion very close to the typical ones in a central field. In this frame, the energy integral for an elliptic orbit with semi-major axis A and eccentricity ε yields

$$\upsilon^2 = \frac{2}{r} - \frac{\varepsilon}{A}, \tag{9}$$

where υ is the absolute value of the normalized velocity (as we consider only symmetric orbits). In the special case of circular periodic orbits of radius r (ε=1, A=r), (9) takes the form $\upsilon = \pm 1/\sqrt{r}$, with the plus sign referring to counterclockwise (direct) motion and the minus sign to clockwise (retrograde) motion with respect to the sidereal system.

Going now to the rotating (synodic) system, its normalized velocity at distance r from the coordinate origin is equal to r in the direction perpendicular to r. Therefore, in the synodic system, the normalized velocity of a circular-like orbit is

$$\upsilon = \pm \frac{1}{\sqrt{r}} - r. \tag{10}$$

From the above equation, it can be understood that four families of periodic orbits are possible to exist. In exact, the term $\pm 1/\sqrt{r}$ corresponds to two different cases: The first one is for r>1 (outside the peripherals), where (10) yields that for direct motion in the sidereal system the motion is retrograde in the synodic system, while retrograde motion in the sidereal system is retrograde also in the synodic system. Hence, in this case, there exist two families of symmetric periodic orbits as in the case of the restricted 3-body problem [1-3]. Eventually, direct family with respect to the rotating system is not possible to exist for N=8, b=2, because the distance of each peripheral from the origin is $r_p \approx 1.15 > 1$. Also, the potential function becomes $V = r^2/2 + 1/r$ and (7) gives $C = r^2 + 2/r - \upsilon^2$, which in its turn becomes from (9)

$$C = \pm 2\sqrt{A(1-\varepsilon^2)} + \frac{1}{A} = \pm 2\sqrt{r} + \frac{1}{r}. \tag{11}$$

From (11) one sees that the absolute value of C is an increasing function of the distance, thus it is expected that the stability index a_1 asymptotically approaches unity [14].

In the second case, where r<1 (inside the peripherals and surrounding the primary) and therefore r_p>r, (9) yields that direct orbits in the fixed system are also direct in the rotating system, whereas retrograde motion in the sidereal system is also retrograde in the synodic system.

IV. Numerical Results

This section is devoted to the presentation of results from the numerical solution of the equations of motion in the planar ring configuration for N=8 and b=2, as described in the last two paragraphs of Section II. Our computations revealed four classes of symmetric periodic motions with respect to the relative position of the trajectory to the primary as well as the peripherals: Orbits around the primary, around the primary and all of the peripherals, around one or more peripherals and among the peripherals. The first three classes of orbits, which are actually planetary-type, have been already identified from the zero-velocity curves in Section III. In addition, the linear stability of the computed orbits is evaluated in terms of the Henon indices and a description of their evolution with respect to the Jacobian constant takes place, including diagrams of characteristics, stability curves and bifurcation point analysis.

A. Orbits around the primary

We mention first the families of periodic orbits, direct and retrograde, that move around the primary. These two families are generated from infinitesimal circular orbits around the primary, as in the case of some classes of the restricted three-body problem [1, 3]. Hence, it can be safely claimed that the initial formation of the family of retrograde orbits corresponds to Poincare orbits of the first type (see [18] for details).

In Fig. 2, the curve marked "a" corresponds to a retrograde orbit with C=5.3, x_0=-0.419, period T=1.587 and a_1=-0.8311. In Fig. 3 top, the characteristic function x=x(C) of this orbit family is shown, and in Fig. 3 bottom the respective stability curve a_1(C) is given. From the latter figure, it is clear that as C decreases the orbits indeed draw away from the primary, as the absolute value of the initial condition x_0 becomes more and more greater than zero. Moreover, when C increases x_0 tends to zero; that is, the orbits shrink to the central primary. In Fig. 3 bottom one sees that for C>10 the stability index is almost equal to 1, thus the orbits are critically stable. For example, for C=15 it is a_1=0.9996 and for C=10 a_1 is 0.9747. As C decreases a_1 also decreases, becomes negative at C=5.78, remaining however absolutely under unity. Then, a_1 becomes -1.00001 at C=5.207, with x0=-0.456, T=1.769, and the other indices are a_2=0.00034, a_3=-0.00011, a combination of values for a_1, a_2, a_3 reflecting a critical point for stability.

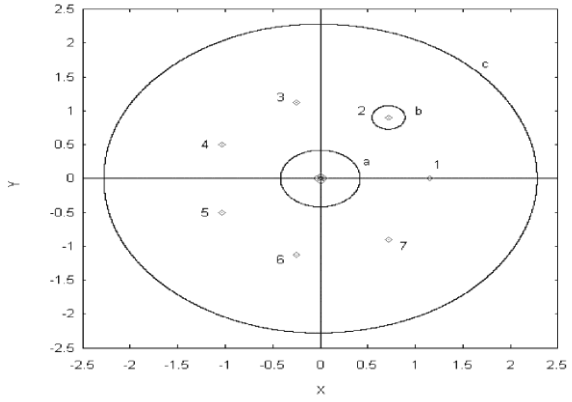

Fig. 2. Planetary-type orbits around the primary (marked with "a"), one peripheral (marked with "b") and all bodies (marked with "c").

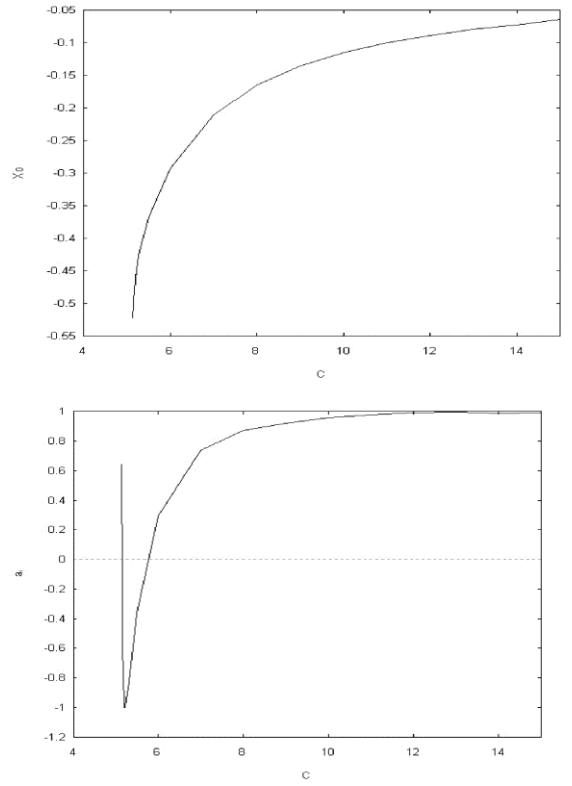

Fig. 3. (Top) Characteristic function x(C) for the family of retrograde orbits of type "a", and (bottom) the corresponding stability curve a_1(C).

The values of a_2 and a_3 at this critical point indicate the occurrence of a period-doubling bifurcation which generates a new family of double-period, symmetric periodic orbits. This bifurcating family is stable in the neighbourhood of the critical point, with two branches in the form of a pitchfork [12]. Some of the double-period orbits from this family were numerically computed with the following parameters: (C=5.2062, x_0=-0.45663, T=3.5432, a_1=0.99947), (C=5.2065, x_0=-0.45655, T=3.5402, a_1=0.99858), (C=5.2068, x_0=-0.45667, T=3.638, a_1=0.99814). The properties of such orbits will be studied more thoroughly in future work. After becoming -1, the stability index starts to increase again until a_1=0.64651 at C=5.136 (and eventually a_1=1 at some nearby value of C). Consequently, as C decreases this family remains stable and,

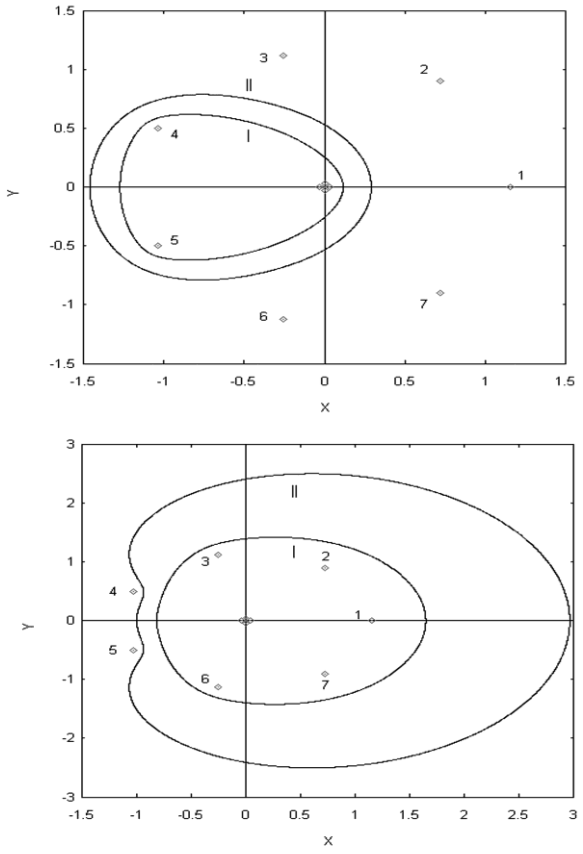

Fig. 4. Families of orbits around the primary and a number of peripherals.

according to all our computations, an elliptic ring of stability develops with horizontal axis between x_0≈-0.01568 (C_1≈50) and x_0≈-0.52274 (C_2≈5.13). For a value of C a little smaller than 5.136 a collision with the peripheral 1 appears.

A decrease of C beyond the aforementioned values leads to families of orbits with different geometric characteristics. In specific, orbits surrounding the primary along with peripheral 1 were found (for example one at C=5.12, x_0=-0.67743, T= 4.3884, a_1=3988), until a value of C where there is a collision, with peripheral 2 this time. Continuing to lower values of C, we computed orbits around the primary and peripherals 4, 5 like the ones presented in Fig. 4 top: (I) C=5.09, x_0=-0.77468, T=6.4906, a_1=7185, and (II) C=5.05, x_0=-0.79012, T=6.9842, a_1=8002. In further decrease of C, a collision of the small body with peripheral 3 occurs, and for even smaller values there appear orbits surrounding all peripherals except 4 and 5 (e.g. C=5.00, x_0=-1.0308, T= 7.6966, a_1=1117) and so on. This kind of orbits is visualized in presented in Fig. 4 bottom.

For the family of direct periodic orbits existing around the central primary, the characteristic curve and the respective stability index diagram are presented in Fig. 5. From the first curve, it is obvious that the orbits evolve in the same way as the retrograde ones. So, for C decreasing they go far from the primary, while if C increases they tend to shrink to it. The second one, the stability curve, brings upon a difference in the stability between the two families. Specifically, for C>12 the stability index is almost equal to 1, making the orbits critically stable. Some indicative values of orbit parameters are (C=12, a_1=0.99994), (C=11, a_1=0.99951) and (C=10, a_1=0.97323).

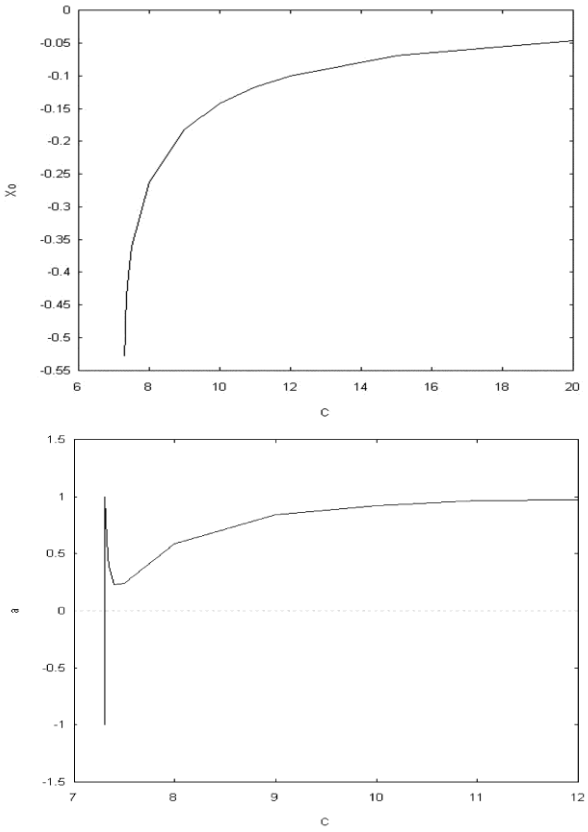

Fig. 5. Characteristic and stability index diagrams of the family of direct periodic orbits existing around the primary.

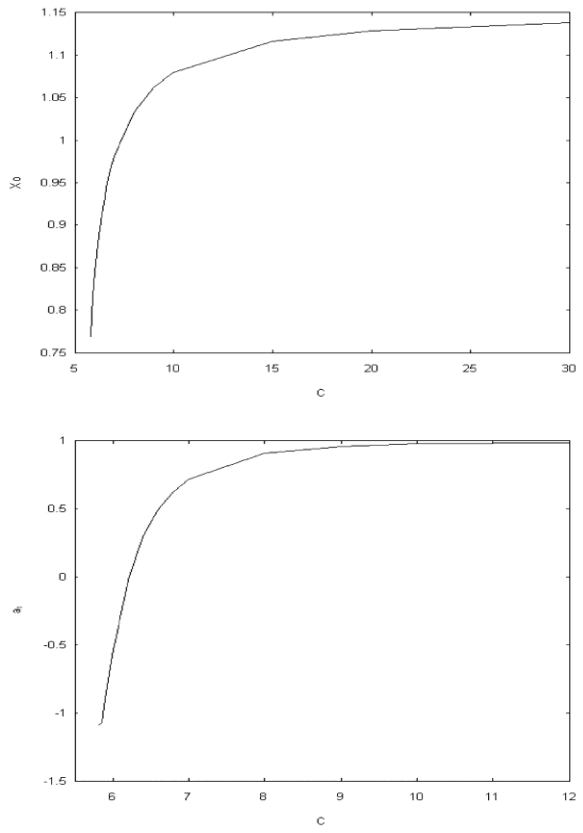

Fig. 6. Characteristic curve and stability index diagram of the family of retrograde periodic orbits existing around one peripheral.

As C decreases more, the stability index also decreases until the value a_1=0.228886 at C=7.4 (x_0=-0.40368). After that, the index starts to increase and reaches the value a_1=1.00002 at the point C=7.309 (x_0=-0.49026), whereas a_2=-0.01005 and a_3=0.01455. This is a critical point where the stability curve is tangent to the straight line $|a_1|$=1, and from the values of a_2 and a_3 one understands that it is a critical point of a bifurcation to a family of non-symmetric periodic orbits of the same period.

Over that point, the evolution is similar to the above one in the retrograde case: a_1 becomes continuously smaller as the Jacobian constant decreases, crosses zero at C≈7.3025 and becomes a_1=-1.00006 at C=7.30087 (x_0=-0.52538, T=6.4372). At this point, the stability curve is tangent to the line a_1=-1 and it is a_2=-0.03285, a_3=0.0005, so we have a bifurcation point leading to double-period orbits which can be straightforwardly computed. This family of direct orbits are stable in the interval from x_0≈-0.01546 (C_1≈50) to x_0≈-0.5252 (C_2≈7.3007), and after C=7.3007 (a_1=-0.68812) a collision with peripheral 1 makes those different from the ones of the family under study.

B. Orbits around one peripheral

In this setting there exist both direct and retrograde orbits, which are generated and rotate around only one peripheral in the same way like the ones presented above. In Fig. 1, the trajectory marked "b" is retrograde periodic orbit surrounding the peripheral 2 with C=7.0, x_0=0.544, T=0.68 and stability coefficient a_1=0.725; another orbit there is for C=6.2, x_0=0.46235, T=1.1904 and a_1=-0.99595. Also, an orbit around peripheral 3 is C=7.00, x_0=-0.4294, T=0.6804 and a_1=0.73367.

In Fig. 6 the characteristic curve and the corresponding diagram for the family of retrograde periodic orbits around peripheral 1 are visualized. From the characteristic (top) it is obvious that, as C becomes smaller, the orbits move away from the peripheral, while for increasing C they move towards it. Fig. 6 bottom shows that after C=12 the index a_1 is almost 1, and so the orbits are critically stable. Indicatively, for C=12 (x_0=1.14034) it is a_1=1.99924 (a_2=-0.0003, a_3=6.50330), while for C=11 it is a_1= 0.99924 and for C=10 it is a_1= 0.97924. As C decreases, the stability index also decreases, crossing a_1=0 at C=6.26, and at C=5.88 (x_0=0.800564, T=1.94511) the indices becomes a_1=–1.00006, a_2=-0.006432 and a_3=0.02131, revealing the existence of a double-period bifurcation point as in the above case. At C=5.8 (x_0=0.76805) it is a_1=-1.09084, and then a collision with one of the neighbouring peripherals arises and the orbits start to surround more than one peripherals (we refer to such orbits later on).

As far as the family of directs periodic orbits is concerned, in Fig. 7 the characteristic diagram and the respective stability curve are presented. From the first one of these, one concludes that the dependence of the orbit properties on the Jacobian constant is similar to that of the retrograde ones seen above: when C decreases the orbits reside far from the peripheral 1, and as it increases these tend to shrink to it, covering less and less area on the x-y plane.

The stability diagram of this family in Fig. 7 bottom implies that there is a difference between the two families as far as their stability is concerned: For this family, the stability index never becomes –1. In specific, for C greater than 20 the index

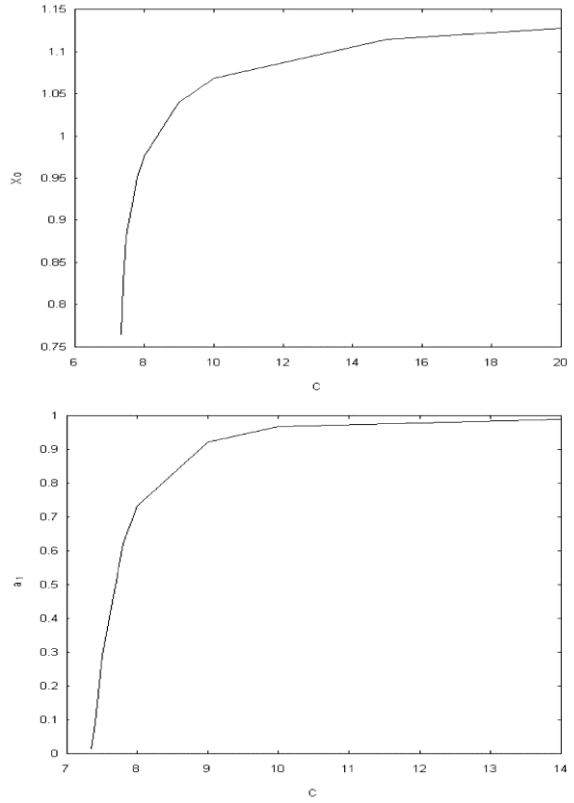

Fig. 7. Characteristic curve and stability index diagram of the family of direct periodic orbits existing around one peripheral.

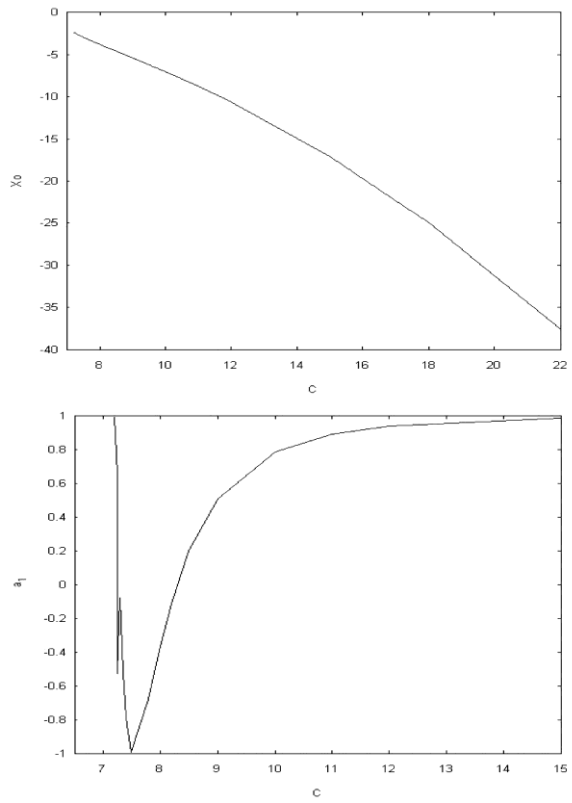

Fig. 8. Characteristic curve and stability index diagram of the family of C-positive retrograde orbits existing around all the peripherals.

a_1 is almost equal to 1 (e.g. for C=20 it is a_1=0.99949 and for C=10 it is a_1=0.96756522). If C continues to decrease, at C=7.35 (x_0=0.7637, T=2.9624) the value of a_1 is 0.0129121, and from then on the orbit collides with one of the neighbouring peripherals and becomes of other type.

Due to the symmetry of the problem, orbits of the type described exist around each one of the 7 peripherals. The behaviour of these orbits is similar to the previous ones, but the new families arising after a collision differ according to the respective peripheral. This is due to the fact that this type of motion is not symmetric to the x-axis of the synodic system but to the x-axis of the local system, which is parallel to the synodic x-axis passing from the respective peripheral.

C. Orbits around all the peripherals

Two families of orbits exist in this case, which are only retrograde in the synodic system and surround all peripherals, similar to some of the classes of the restricted three-body problem [3]. The first one, visualized in Fig. 1 (marked "c", C=7.2, x_0=-2.279, T=14.356, a_1=0.9991), comes from nearly circular trajectories far from the peripherals for large positive C, and the other is created also from circle-like orbits far from the peripherals with C being negative. As C varies, the orbits of the two types close up to the peripherals and get an elliptic shape, until a value of C where there is a collision with one of the peripherals. In Fig. 8 we give the characteristic curve and the stability diagram for the positive-C family of retrograde orbits. From the characteristic it is obvious that when C decreases the orbits close up to the ring configuration, whereas for increasing C the orbits draw away from the peripherals.

Fig. 8 bottom shows that for C>14 the index a_1 takes values very close to unity, therefore the orbits are critically stable. Indicatively, for C=14 it is a_1=0.99878, for C=13 it is a_1=0.995813, while for C=12 we have a_1=0.942419. With C decreasing, a_1 varies remaining absolutely smaller than 1 and becomes equal to zero at C≈8.57. It gets the value a_1=-0.99241 at C=7.5 (x_0=-2.9532, T=9.97031). At this transition point, in which the stability curve is tangent to the straight line a_1=-1, and a_2=-0.37294, a_3=0.03962, a bifurcation towards a double-period family takes place. The bifurcating family, which has two branches in the form of a pitchfork, is stable in the region of the critical point. After this point, as C decreases the stability index begins to increase and at C=7.2 (x_0=-2.2845, T=14.5454) we have a_1=0.999101. At this new critical point, where a_2=-0.07164 and a_3=0.01185, bifurcates a new family of non-symmetric simple periodic orbits.

As C decreases more and more, the index a_1 continuously decreases and orbits with a rough edge arise at C=7.1, x_0=-1.90165, T=18.559 and a_1=-3866.56. This edge is located near the Lagrangian point of gravitational equilibrium for the N-body system, which has coordinates (-0.98,1.23) (see [10, 11] for details). For even smaller values of C, the existing periodic orbits still surround all the peripherals presenting a curving near their launch point at C=7.05, x_0=-1.7437, T=13.0834 and a=-98.97 until the small body collides with peripheral 3. After that, a new type of orbits arises; these orbits leave out peripherals 3, 4, 5 and 6, presenting cusps at these positions at C=7.02, x_0=-1.71587, T=19.719, a=-33817.3 and becoming strongly unstable (this type of orbits will be studied, among others, in the following section).

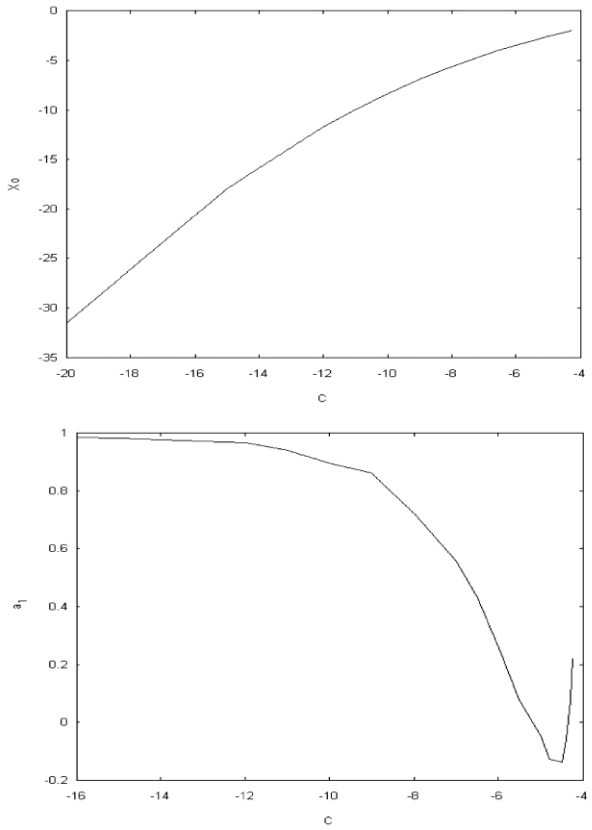

Fig. 9. Characteristic curve and stability index diagram of the family of C-negative retrograde orbits existing around all the peripherals.

In Fig. 9 the characteristic diagram of the family of orbits existing for negative C and the stability index a_1 as a function of C are visualized. A similar behaviour to the family of orbits with positive C, presented above, is found, however with a different direction in monotony: Here when C decreases the orbits draw away from the ring, while when it increases x_0 decreases absolutely, thus the orbits draw near the peripherals.

The stability index never becomes -1, and so a bifurcation to a double-period family does not occur. In particular, for C less than -16 the index is very close to 1, making the orbits critically stable: For C=-16 the index a_1 is 0.99702364, while for C=-12 it is 0.96610281. As C grows, the absolute value $|a_1|$ always remains less than 1, becoming at first equal to zero at C≈-5.3, and then getting the value -0.13918 at C=-4.5 (x_0= -2.1751, T=2.9266). This value is a minimum, as afterwards a_1 rises again, becoming equal to a_1=-0.06045 for C=-4.4 and a_1=0.07522 for C=-4.3. In the end, after C=-4.25, where x_0=-1.8998, T=3.5142 and a_1=0.22233, there is a collision orbit with one of the peripherals, the orbits become very unstable and differ from the ones before.

D. Orbits among the peripherals

The last type of motion analysed comprises of the retrograde orbits that twist among the peripherals. Their shape and location on the x-y plane, as well as other geometric and dynamic properties, vary depending on their initial conditions. As an example, we mention that our computations showed orbits that surround two or more peripherals and also exhibit a curving at the central body or at one or more peripherals.

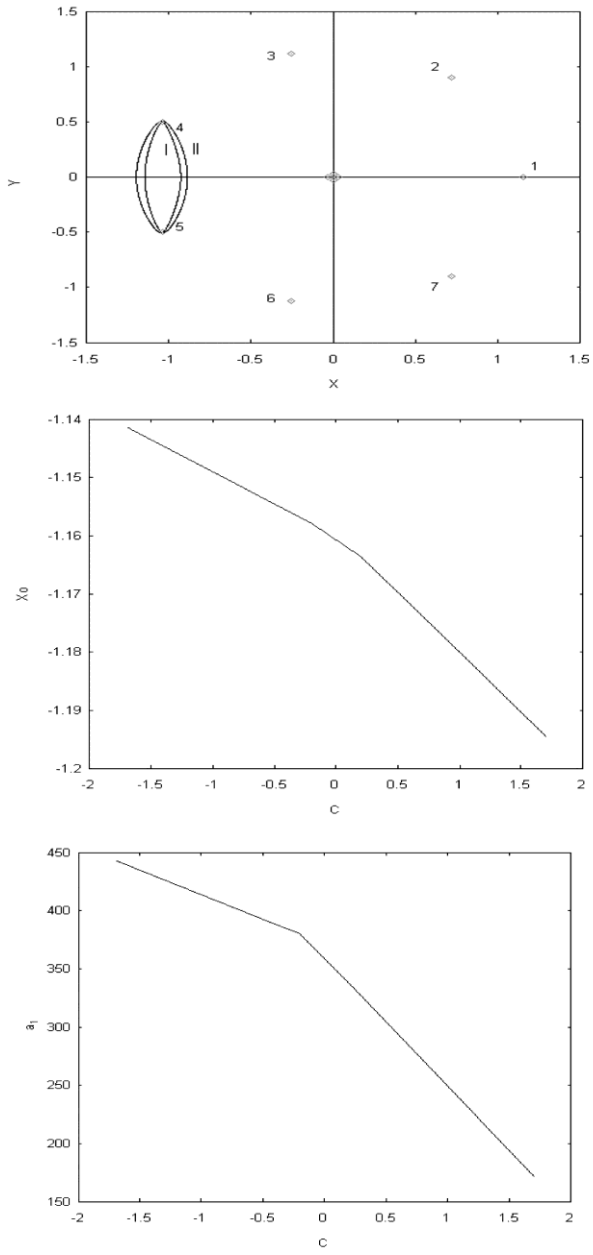

Fig. 10. The family of retrograde orbits existing around the peripherals 4, 5, together with its characteristic curve and the stability index diagram.

At first, regarding the retrograde motion around two peripherals, in Fig. 10 we show orbits around the peripherals 4 and 5, as e.g. the orbit (I) with C=-1.700, x_0=-1.141, T= 0.61 and a_1=443.2. Also, in the same figure we plot the x_0-C and the a_1-C curves, which yield that the specific family of orbits is unstable, with the very large values of the stability index having a minimum a_1=43.82 at C=0.95, x_0=-0.46785 and increasing again. As C decreases, the orbits draw near more and more to the two peripherals and for a certain value of C a collision appears with one of them.

For higher values than C=1.700 (where x_0=-1.194, T= 0.78 and a_1=171.8), we have computed a number of other families of orbits. At first, as C increases and after a collision with the central body, there are orbits surrounding also the central body. This is actually a different family of retrograde periodic

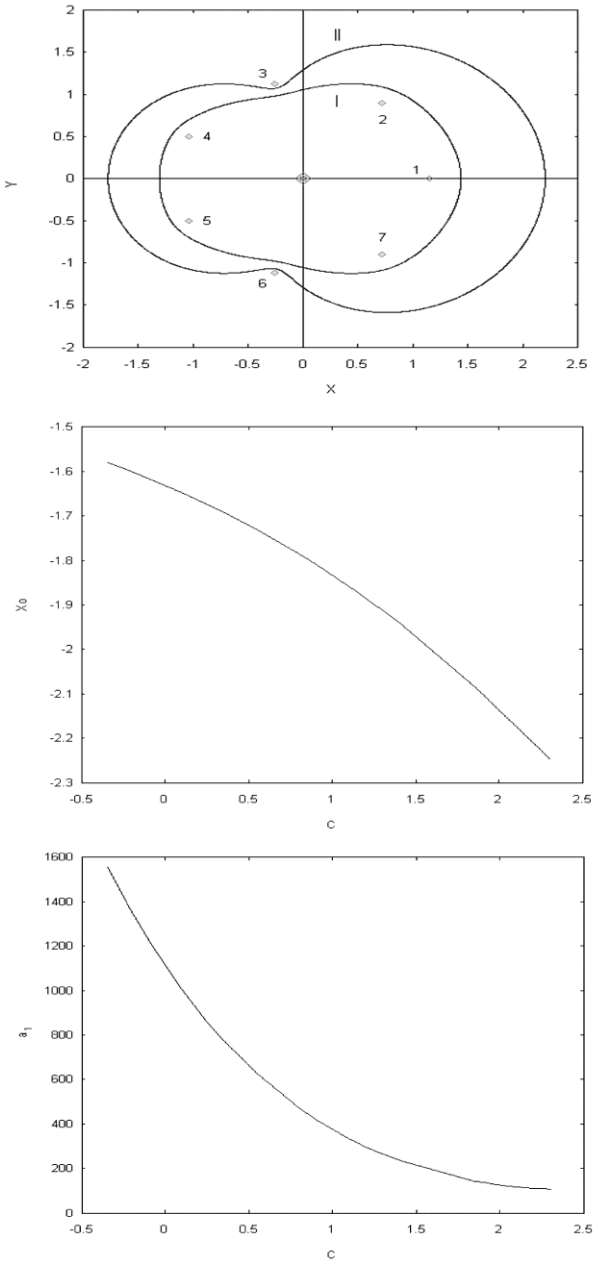

Fig. 11. The family of retrograde orbits leaving out the peripherals 3 and 6, together with its characteristic curve and the stability index diagram.

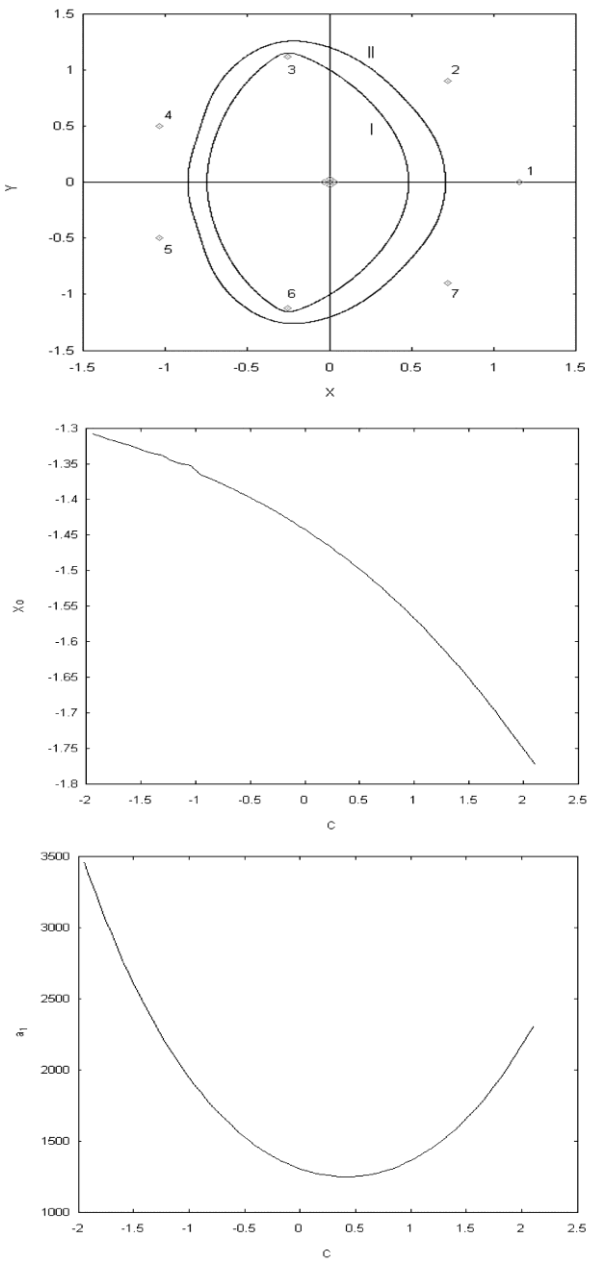

Fig. 12. The family of retrograde orbits surrounding the peripherals 3 and 6, together with its characteristic curve and the stability index diagram.

orbits around the primary and peripherals 4, 5 with respect to the one which has been presented previously (see Fig. 4). An orbit of this family has been computed for C=0.500, x_0=-1.271, T= 1.104 and a_1=180.9. The evaluation of the function a_1(C) has made clear that the family is very unstable, and the index a_1 has a minimum value 30.7 at C=2.00, x_0=-1.458. As C decreases the orbits approach more the internal peripherals, while moving to the external ones as C increases.

Increasing C even more we finally collide with peripheral 1, and afterwards we found orbits like the one shown in Fig. 11, which surround all the bodies of the ring except the symmetric peripherals 3 and 6. The characteristic and stability diagram of this family are also given in Fig. 11. The orbits of this family are unstable, moving more towards the internal or external peripherals as C decreases or increases respectively.

Further computations associated with the unstable character of new families of retrograde periodic orbits. In Fig. 12 we analyse a motion that surrounds the peripherals 3 and 6 as well as the primary, for C=-1.450, x_0=-0.746, T=1.76 and a_1=2235.9, and in the same figure we provide the curves x_0-C and a_1-C. It is evident that the curve a_1(C) appears a minimum, equal to a_1=1472.64, at C=1.15, x_0=-0.8183. As C decreases, the orbits approach more and more the two peripherals and after a collision with either one of them we found orbits similar to the one shown in Fig. 11, for C=2.50, x_0=-0.648, T= 4.02 and a_1=262.8. By increasing C, and after C=2.50 (x_0=-0.863, T= 2.7 and a_1=1808.5), we get orbits similar to that of Fig. 12 again. These two classes are very unstable and as C changes, the orbits of the families move more to the internal/external peripherals as C decreases/increases.

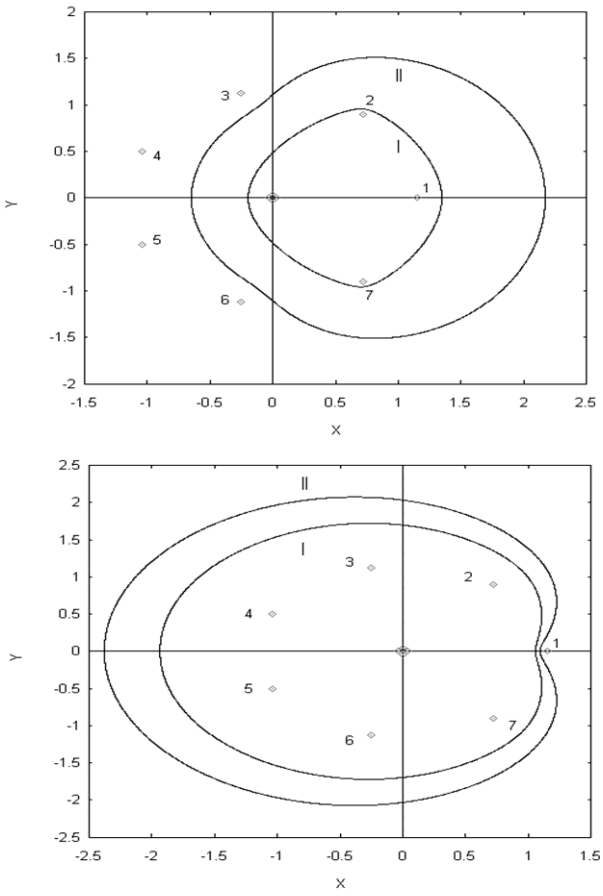

Fig. 13. Trajectories from the families of retrograde orbits that surround all bodies except peripherals 3-6 (top) or peripheral 1 (bottom).

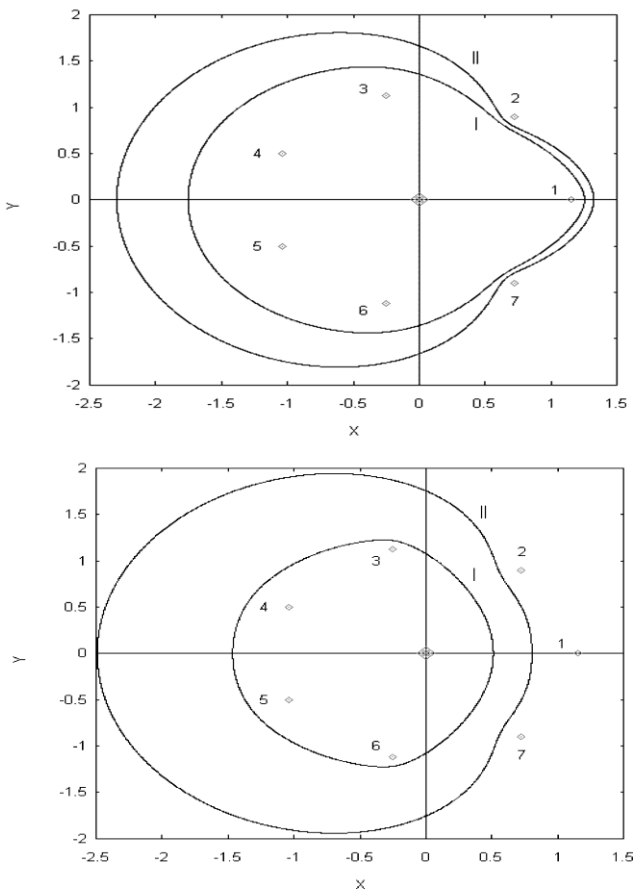

Fig. 14. Trajectories from the families of retrograde orbits that surround all bodies except the peripherals 2, 7 (top) or 1, 2, 7 (bottom).

In the same manner we discovered four new families of retrograde periodic orbits which are all unstable. The orbits of these families are presented in Figs. 13 and 14. In Fig. 13 bottom we observe that the orbit curves at the peripheral 1, surrounding all the rest bodies, with C=-1.95, x_0=-1.934, T=3.4 and a_1=53.7. This family was found for negative values of C. The stability curve has a minimum a_1=50.2 at C=-1.6 (x_0=-2.0875). As C decreases the orbits close up more and more to all the peripherals, except 1 from which they move away, while the curving smoothens.

Fig. 13 top shows an orbit for C=2.309, x_0=-0.521, T=1.25 and a_1=641, curving at the peripheral 1 and surrounding only the symmetric peripherals 2 and 7 and the central body. The curve a_1(C) appears a minimum a_1=57.6574 at C=0.1 (x_0=-1.84854). As C decreases the orbits approach more and more the peripherals 2 and 7 and move away from peripheral 1, while the curving smoothens. We should note that the aforementioned orbits have similar form with some of the classes of the restricted three-body problem [1-3].

An orbit with initial conditions C=-0.90, x_0=-1.75, and T=3.07, a_1=929, is shown in Fig. 14 top. The orbits of this family surround all bodies except peripherals 2 and 7. They present similar behaviour as above: As C decreases the two symmetric rough edges that exist at the peripherals 2 and 7 smoothen and the orbits move away from them more and more approaching the peripherals 1, 3, 4, 5 and 6. The stability index has a minimum a_1=57.7 at C=-0.05, x_0=-1.83276.

The last family has orbits of similar form with the previous ones, that do not surround the peripherals 1, 2 and 7 (Fig. 14 bottom), for C=2.050, x_0=-2.491, T=4.64 and a_1=381.3. As C decreases they move more and more near to the peripherals 3, 4, 5 and 6 and far away from the peripherals 1, 2 and 7. Also, the two symmetric curvings at the peripherals 2 and 7 become more and more smooth.

V. Conclusion

In this paper we have studied the geometry and dynamics of the simple, symmetric periodic motions in the N-body ring problem for N=8 and b=2, with the following main results:

(i) A theory investigation, under certain approximations, ascertained four families of symmetric periodic orbits, which we verified also numerically: Two families of periodic orbits around the central body, one sidereal retrograde (also synodic retrograde) and the other sidereal and synodic direct. Also, two families around all peripherals, one retrograde in both the rotating and the fixed system and three direct in the fixed system and retrograde in the rotating one.

(ii) For the retrograde and direct periodic orbits around the central body we can say that as the Jacobian constant increases the orbits approach the central body and shrink to it, while as C decreases the elliptical-shaped orbits go far from the central body more and more increasing in size. The decrease of C leads us in finding different families, the orbits of which perform a curved/twisted motion among the peripherals.

(iii) The stability curves of the retrograde and direct periodic orbits appear bifurcation points. At these critical points, the curves are tangent to the straight line a_1=-1. So, there are new bifurcating families of symmetric double periodic orbits with two branches in the form of a pitchfork. The bifurcating families are stable in the neighborhood of the critical points. Also, there are other bifurcation points with $|a_1|$=1. Thus, we have here bifurcations with new families of non-symmetric simple periodic orbits of the same period. These two families of simple periodic orbits are stable in an interval [C1,C2], and rings of stability develop between C1=50, C2=5.13 for the retrograde orbits and C1=50, C2=7.3007 for the direct orbits.

(iv) A characteristic of almost all the previous families that exist among the peripherals, is that when C decreases the orbits draw into the central primary. Also, another important conclusion is that, as far as the stability curves are concerned, all of these families are strongly unstable. The stability index takes in all cases large positive values (a>>1), having a minimum value for certain initial conditions values and then increasing again. This is probably due to the gravitational effect of the peripherals to the small body's motion.

The above results lead to the conclusion that the motion of the small body, after a while, will escape and will be bound around all the peripherals, around the central body or around one peripheral, depending on the initial conditions. Also, the stability ring regions of retrograde periodic orbits are larger than those of direct ones; thus, the retrograde orbits around the formation are more stable than the direct ones. This is a very interesting property to consider in astronomical applications.

It is therefore understood that the first three groups of families of planetary-type periodic orbits present important astronomical and astrophysical interest. A further study with a more solid conclusion might elaborate on the importance of the current work or suggest applications and extensions.

REFERENCES

[1] G. Mittag-Leffler, "The n-body problem", *Acta Mat.*, vol. 7, 1886.

[2] J. Hadjidemetriou, "Stability of periodic planetary type orbits of the general planar *N*-body problem", *Cel. Mech.*, vol. 16, p. 61, 1977.

[3] V. Szebehely, *Theory of orbits.* New York: Academic Press, 1967.

[4] K. G. Contopoulos, *Order and Chaos in Dynamical Astronomy*. New York: Springer, 2002.

[5] F. R. Moulton, *An Introduction to Celestial Mechanics*. Cambridge: Dover Publications, 1970.

[6] K. G. Hadjifotinou and T. J. Kalvouridis, "Numerical investigation of periodic motion in the three-dimensional ring problem of N bodies" *Int. J. Bifurcation Chaos*, vol. 15, p. 2681, 2005.

[7] A. Elipe, M. Arribas and T. J. Kalvouridis, "Periodic Solutions in the Planar (n+1) Ring Problem with Oblateness", J. *Guid. Control Dyn.*, vol. 30, p. 6, 2007.

[8] T. J. Kalvouridis, "Multiple Periodic Orbits in the Ring Problem: Families of Triple Periodic Orbits", Astroph. Space Sci., vol. 277, p. 579, 2001.

[9] T. J. Kalvouridis and K. G. Hadjifotinou, "B ifurcations from planar to 3-d periodic orbits in the ring problem of n bodies with radiating central primary", *Int. J. Bifurcation Chaos*, vol. 21, p. 2245 (2011).

[10] A. D. Pinotsis, "Evolution and stability of the theoretically predicted families of periodic orbits in the N-body ring problem", *Astron. Astrophys.*,vol. 432, p. 713, 2005.

[11] A. D. Pinotsis, C. S. Tsironis and T. J. Kalvouridis, "Symmetric periodic motion in a ring problem", in *Proc.5th Hellenic Astron. Conf., 2001.*

[12] S. Wiggins, *Introduction to applied nonlinear dynamical systems and chaos*. NewYork: Springer, 2003.

[13] W. H. Press, S. A. Teukolsky, W. T. Vetterling and B. P. Flannery, *Numerical Recipes: The Art of Scientific Computing*. New York: Cambridge University Press, 2003.

[14] M. Henon, *Ann. Astrophys.*, vol. 28, p. 992, 1965.

[15] A. D. Pinotsis, "Bifurcations, stability and universality of families of periodic orbits in the restricted three-body problem", *Astron. Astrophys.*, vol. 159, p. 231, 1986.

[16] V. Szebehely, *Astron. Journal*, vol. 68, p. 147, 1963.

[17] T.J. Kalvouridis, "On a property of zero-velocity curves in N -body ring-type systems", *Planet. Space Sci.*, vol. 52, p. 909, 2004.

[18] H. Poincare, *Les méthodes nouvelles de la mécanique celeste*. Paris: Gauthier Villars, 1899.

Christos S. Tsironis received the Physics degree from the National and Kapodistrian University of Athens, Greece in 1999, the M.Sc. degree in Physics from the National and Kapodistrian University of Athens, Greece in 2002, and the Ph.D. degree from the Aristotle University of Thessaloniki, Greece, in 2007.

From 1999 to 2001 he was with the Nonlinear Dynamical Systems Analysis Group, National and Kapodistrian University of Athens. In 2003 he joined the Plasma Astrophysics Group, Aristotle University of Thessaloniki, where he is currently a part-time post-doctoral associate. He has been a research associate of the Association EURATOM-Hellenic Republic since 1999, and in 2008 he joined the Electro-Optics Group, National Technical University of Athens, where he conducts the other part of his post-doctoral research. His research interests include nonlinear dynamics, wave physics and plasma physics with applications in astrophysics and thermonuclear fusion.